A Novel Full Waveguide Band Orthomode Transducer

Gopal Narayanan[1], and Neal R. Erickson

Department of Astronomy
University of Massachusetts
Amherst, MA 01003

Abstract

At millimeter and submillimeter wavelengths, cryogenically cooled receivers based on SIS and HEB technologies are approaching the quantum limit in noise temperature. Further increase in sensitivity can be obtained by using dual-polarized operation. One of the principal components of a dual-polarization receiver is a polarization diplexer or orthomode transducer (OMT). Traditionally the OMT used in radio astronomy receivers is the wire grid, which can be large and bulky. A waveguide based OMT, on the other hand, can be integrated with the mixer blocks and cryogenically cooled thereby reducing ohmic losses. A waveguide based OMT also lends itself well to integration into focal-plane array receivers. In this paper, we present the design of a novel OMT that can be constructed using conventional split-block techniques. The design is based on the proposed Bϕifot OMT by Wollack [1], but has been considerably modified to (a) make it easy to fabricate, and (b) make it scalable to $\sim$ 1 THz. The return loss is -20 dB or better over a full waveguide-band ($\sim$ 40% bandwidth), and the cross-polarization and isolation are better than -70 dB. Design details of a W-band OMT are presented.

1 Introduction

An orthomode transducer (OMT) is a device that separates orthogonal polarizations within the same frequency band. In the literature, OMT's are called by various other names such as polarization diplexers, dual-mode transducers, orthomode junctions or orthomode tees. With receiver noise temperatures of waveguide-based SIS and HEB mixers approaching a few times the quantum limit, further increase in sensitivity can be obtained using dual-polarized operation. In radio astronomical applications, the conventional way to separate orthogonal polarizations is the wire-grid diplexer, which is a quasi-optical device that consists of free-standing parallel wires. The polarization with the E-field parallel to the wires is reflected, while the component orthogonal to the wires is transmitted through. However, the wiregrid polarization diplexer is large and bulky. If we desire the mixers for both polarizations to reside in one cryostat, the wiregrid should preferentially be inside the dewar, which correspondingly increases the size of the required dewar. A broadband waveguide-based OMT would be a preferable alternative as it would much smaller, and it would be a good match to available high-performance dual-polarized broadband corrugated feedhorns. A

[1]e-mail: gopal@astro.umass.edu

waveguide based OMT also lends itself well to integration into focal-plane array receivers. In this paper, we present the design of a full-waveguide band OMT for the W-band, which is scalable to 1 THz.

2 General Considerations for OMTs

With improved fabrication techniques [2,3,4], high-quality waveguide blocks can be made to 1 THz and beyond. One of the principal requirements in our design is the scalability of the design to terahertz frequencies. An OMT used for radio astronomy purposes should satisfy several important requirements: (1) A return loss of $\sim$ 20 dB or better for a full waveguide band ($\sim$ 40% bandwidth). (2) Isolation between the two orthogonal polarization ports of better than 40 dB. (3) Cross-polarization term should be less than 40 dB. Cross-polarization for a given polarization port is the amount of signal present from the orthogonal polarization. One of the driving goals of an OMT design should be that the cross-polarization introduced by the OMT should not exceed that produced by the optics and feedhorn that precede it in the system. (4) Low Insertion Loss. Since the OMT will be operated cryogenically the ohmic losses are less important that for room temperature operation. (5) The design should be scalable to 1 THz. The fabrication of the OMT should lend itself to established split-block techniques.

For any waveguide device, the broadband operation of the device is tied to its symmetry properties. Symmetrical or non-symmetrical transitions in waveguides produce higher order modes. Most of the higher modes are evanescent and do not propagate. However, uncompensated higher order modes store reactive energy which prevents the broadband operation of the device. What sorts of higher order modes are produced often dictates the broadband isolation and input match of waveguide devices. To design a broadband device, it is necessary to design the transitions such that only even-order higher modes are produced, because they are easier to compensate. A waveguide device is defined as symmetrical if different transitions cause the dominant mode to only generate symmetrical (even-order) higher modes. A device is defined as non-symmetrical if the dominant mode, in addition produces odd-symmetrical higher order modes.

Bϕifot classified waveguide-based OMTs into three groups [5,6] based on their increasing symmetry. Class I represents the simplest and most common approach, with one main arm for one mode and one orthogonal sidearm for the other mode. The main arm mode is symmetric while the sidearm mode is not. An example of such an OMT is that used in [7], where the H-bend in the sidearm breaks its symmetry, resulting in narrower percentage bandwidth ($\sim$ 20%). The Class II configuration OMT is more complex. Here there is one main arm, but the side arm is split into two symmetrical parts from the main arm. An example of this sort of device is that presented in [5] and implemented by Wollack [1]. In this device, the main arm mode sees a symmetrical device as in the Class I equivalent. In addition, the side arm also sees symmetrical splitting and combining junctions. The symmetrical nature of this splitting and combining makes it possible to achieve a good broadband match even for the side arm mode. The Class III OMTs are even more complex, with both the main and side arms split into two symmetrical parts. The splitting junction essentially forms a classic turnstile junction whose matching properties have been well studied [8]. Since the splitting junction is symmetric both in the main and side arms, higher order symmetric modes will naturally be canceled in both arms, and thus these OMTs should have a natural broadbanded match and isolation performance. However, this class of OMT is very complex and hence expensive to fabricate.

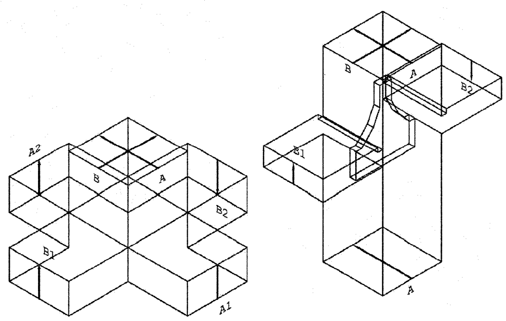

Figure 1: (a) The six-port Classic Turnstile Junction. A and B denote the two ports at the input for the orthogonal polarization. (b) Folded Turnstile Junction, which becomes a Class II OMT. Ports A1 and A2 are folded together.

The Bϕifot junction [5] is a Class II OMT, but it can be thought of as a turnstile junction where two of the ports have been folded parallel to the common port (see Figure 1). The two ports that form the main arm are separated by a metal septum, recombined into square waveguide and then transformed into a standard full-height waveguide. The two symmetric side arms remain the same as in the Class III turnstile-type OMT. For the polarization meant for the side arms, the septum can be thought of as back-to-back "mitered" bends which feeds the symmetric side arm ports. A WR-42 OMT based on the Bϕifot design was made and tested by Wollack [1]. In Bϕifot's design, pins are placed at the entrance apertures of the side arms. There are a pair of such pins for each sidearm. These pins act as capacitive posts. From the perspective of the main arm, these pins tune out the discontinuity of the holes created by the side arms in the main waveguide. From the perspective of the side arms, these pins along with the shape of the septum serve to tune out the dispersive reflective termination that is created by the septum in the main arm. While the pins provided adequate match for the OMT, their small diameters (0.127 mm for the 3 mm band) and the complexity of assembly of the pins in the block make them unsuitable for scaling the OMT to terahertz frequencies. In this work, we replaced the pins with capacitive steps at the side arm apertures (see Figure 1) which are easy to fabricate in-situ with the waveguide block, and work as effectively as the pins do.

3 OMT Design

3.1 Design Methods

Most parts of the OMT design was carried out using CST Microwave Studio (CST MWS) [9]. CST MWS is based on the finite integration (FI) method, which is a one-to-one translation of Maxwell's equations into a discrete space formulation without simplification or specialization. As a general approach its theoretical framework has been developed by the likes of particle accelerator designers for over three decades, and hence is a robust design tool. The FI method works explicitly in the time domain, and hence a full broadband simulation can be performed in one single solver run. MWS is well suited for electrically large structures and features a powerful, parametric drawing editor to lay out the structures. It also comes with a built-in optimizer which was used heavily to optimize the geometry of the septum and the dimensions of the capacitive waveguide steps. While most of the design was carried out in CST MWS, some critical portions such as the junction part of the OMT were also simulated with Agilent's HFSS [10]. The HFSS results verified the predictions of CST MWS, and hence the final results and optimizations were derived using the latter.

3.2 OMT Junction

The design of the complete OMT was done in several steps. First the OMT junction where the main and side arm waveguides meet was designed. The two orthogonal polarizations A and B (see Figure 1b) travel through the input square waveguide (WR-10 dimensions 2.54×2.54 mm). The septum lies in the split block plane at the junction. Polarization A travels straight through the main arm, while polarization B is split through the side arms and later recombined. The design and optimization of the septum and capacitive waveguide steps were carried out separately for both polarizations. Full symmetry considerations were used. Only one quarter of the structure shown in Figure 1b was simulated with magnetic and electric walls on the planes of symmetry being applied to reduce the problem size and solution times. The optimization was carried out for best input match over the 75 – 110 GHz for both polarizations by varying a variety of physical dimensions of the junction. The parameters that were varied included the size of the aperture for the side arm (the side arm waveguide height), length and width of the capacitive step, and several geometrical dimensions of the septum. The metal septum was treated as a perfect conductor. Both for simplicity of optimization and for fabrication ease, the septum was modeled as a simple shape with straight edges. Due to the requirements that the design be scalable to a THz, the design was pushed towards geometries where the thickness of the septum was greater. The final optimized design for the junction is shown in Figure 2. Figure 3 shows the input match at the OMT junction for the main arm and side arm polarizations for the chosen geometry.

The side arm waveguide is 0.813 mm (0.032") in height, with the capacitive step in the waveguide measuring 0.208×0.165 mm in dimension. The requirements of good input match for the two polarizations have an opposite dependence on the thickness of the sep-

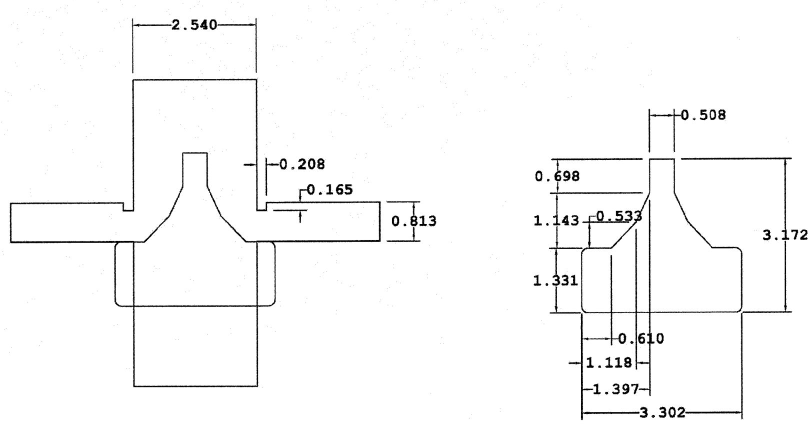

Figure 2: (a) Split-block view of the optimized OMT junction. All dimensions are in millimeters. (b) View of the Septum with some relevant dimensions. The septum is 0.254 mm thick for the W-band OMT.

tum. The bandwidth of good match for the side arm polarization (polarization B) increases with increasing septum thickness. For this polarization, increasing septum thickness makes the septum look more and more like back-to-back mitered bends. For the main arm (polarization A), the bandwidth of good match reduces with increasing septum width. A thin septum produces less discontinuity than a thick septum. The dimensions and geometry of the capacitive step acts as an additional variable in adjusting the match. The optimal thickness of 0.254 mm chosen here for the septum represents a good compromise for the two polarizations, while still remaining an easy enough junction to fabricate.

3.3 E-Plane Bend Across Split Block

In the main arm, polarization A travels through the 1:1 square waveguide and is then transformed into a full-height rectangular waveguide. The transformer is followed by an E-plane bend across the split-block to bring the port out orthogonal to the side-arm port. The square to rectangular transition is accomplished using a 3-section transformer. The transformer is immediately followed by the E-plane bend. The bend itself consists of two steps, both below the split block plane (see Figure 4). In the top block of the split-plane, a full-height rectangular waveguide brings out the main arm port to the outside world. The rectangular waveguide in the top block is hard to machine (it would have to be punched or fabricated as a cylindrical insert and pressed and soldered prior to milling the rest of the features in the top half). In view of this, we designed an oval waveguide which can be directly machined with an end-mill. The oval waveguide uses full-radius corners (0.635 mm), and has a = 2.79 mm (10% increased). Figure 4c shows that the reduction in bandwidth of match for using oval waveguide is minimal. The distance from the OMT junction shown in Figure 2 and the transformer E-plane bend shown of Figure 4 is 0.94 mm. This distance

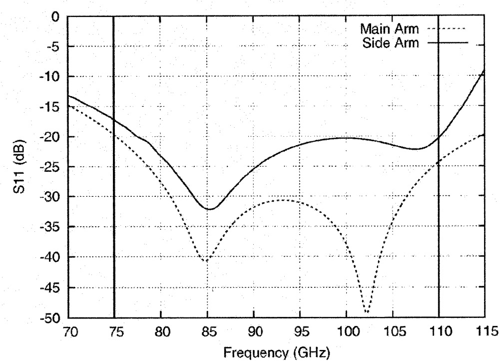

Figure 3: Input match (S11) in dB for the polarizations in the main and side arms for the OMT junction. The side arms match is worse because the side arm sees less symmetry than the main arm. Nevertheless, between 75 – 110 GHz, the match is seen to be at least as good as the required 20 dB.

was optimized in a linear circuit simulator [11] by using ideal rectangular waveguide transmission line sections between the de-embedded S-parameter equivalent networks from the OMT-junction and the transformer section.

3.4 E-Plane Combiner for Side Arm

The two side arms are made to bend around the main arm features through a pair of E-plane bends and are then recombined into a full-height rectangular waveguide which emerges on the opposite side of the square input waveguide of the block. A full-height to full-height waveguide E-plane power divider/combiner design has been recently presented by Kerr [12]. In the Kerr design, the two incoming full-height rectangular waveguides meet in a square waveguide section which is then transformed back into rectangular waveguide. The resulting combiner is physically quite long ($\sim$ 8 mm for W-band). We designed a very simple power combiner with excellent performance across a full waveguide band to combine two side arm waveguides (with a height of 0.813 mm each) to full-height waveguide. This combiner has the advantage that its length is quite small (2.54 mm). Figure 5 shows the cross-sectional view of the resulting combiner and its predicted performance.

At the junction of the combiner, the two waveguide arms are a little over half-height (0.762 mm high). There is a broad pedestal in the middle of the combining junction. Surprisingly in this reduced height guide, such a simplified geometry works as well as the more complex E-Plane Y junction shown in [12]. This combining junction, which can be thought of as an E-Plane Tee power divider can also be used for power division or combining for full-height to full-height waveguides. In Figure 5b, the input match for our E-Plane Tee power combiner is compared against the full-height Kerr Y combiner, and a slightly modified version of the E-Plane Tee combiner for full-height waveguide. Especially for power

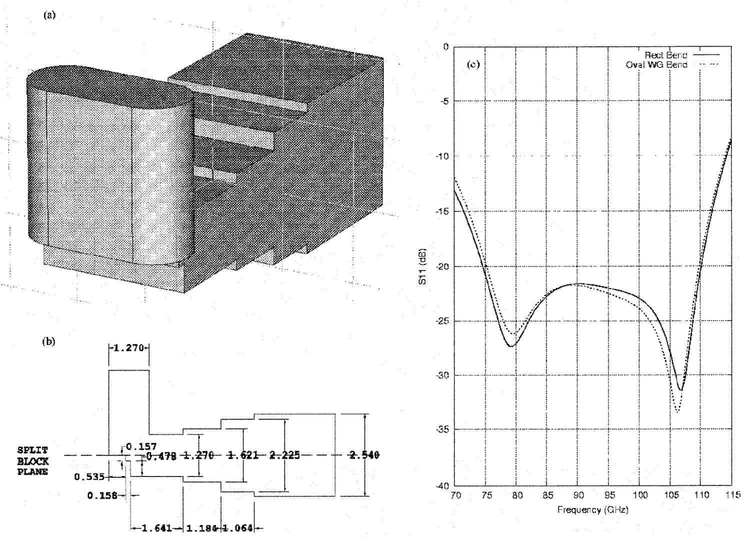

Figure 4: Square to rectangular transformer and E-plane Bend Across Split-block plane. (a) Isometric view of the transformer and E-plane bend; (b) Cutout view with dimensions. All dimensions are in mm; (c) Input match for the transformer and E-plane bend. The two curves show the change in the match from using rectangular and oval waveguides in the top half of the split plane.

combination in reduced height geometries, it can be seen that the E-Plane Tee is simple, compact, and has excellent performance. Even for full-height waveguides, the E-plane Tee has acceptable match over a full waveguide band.

3.5 OMT Predicted Performance

Figure 6 shows the isometric inside and outside view of the OMT with all the individual sections added together. A full simulation of the entire structure leads to the predicted performance curves shown in Figure 6c and d.

The input match is seen to be ≤ -20 dB across the 75 – 110 GHz band. Isolation and cross-polarization terms are more than 75 dB down across the band (not shown in the figure). We also simulated the effect of bending the septum or not having the septum properly centered in the center of the junction. Even when the septum is moved a full 0.127 mm (half its thickness) from the split-block plane, simulations show that the input match is only degraded by $\sim$ 2 dB, while the isolation and cross-polarization terms are still better than 50 dB down. To gauge the effect of conductor losses in the OMT, the perfect conductors used in the simulation were replaced with a conductor of conductivity 2×10^7 S/m. This yielded a maximum insertion loss of $\sim$ 0.1 dB and $\sim$ 0.2 dB in the band, with a typical loss of $\sim$ 0.06 dB and $\sim$ 0.15 dB for the main arm and side arm polarizations

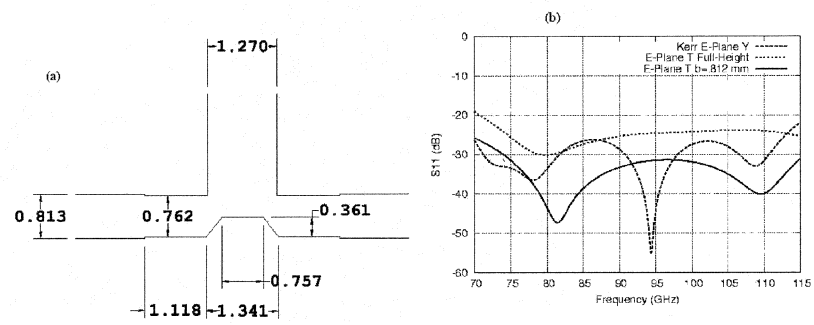

Figure 5: E-Plane Combiner Junction. (a) Dimensional details of split-block view of the E-plane Tee combiner. (b) Input match of the combining junction. Shown for comparison are two more S11 curves. The Kerr E-Plane Y combiner for full-height waveguide and our full-height E-plane Tee combiner design with one additional section added to transform the two input sides to full-height waveguide.

respectively.

At the time of this writing, the septum has already been made, and a test WR-10 block is being fabricated. Tests of the prototype OMT will be reported in a forthcoming ALMA memo.

4 A Scalable and Machinable Design

The Wollack NRAO OMT design had very tight mechanical tolerances and difficult assembly, and is not suitable for scaling much above $\sim$ 150 GHz. The new OMT design presented here avoids these problems. One of the significant advantages of this design is that the waveguide pins (0.127 mm for W-band) that was used in the Wollack design has been replaced with simple capacitive steps. The new design also has a septum that is over four times thicker than that used in the Wollack design, which considerably eases the task of assembly and handling of the septum. The compact split-block design is well suited to CNC machining. The design as presented for the W-band can be scaled to 500 GHz with little difficulty in machining. Slight modifications in the design and re-optimizations should yield machinable designs with acceptable performance even to 1 THz. In the OMT junction, some of the septum's geometrical parameters can be traded off against the waveguide step capacitor, whose dimensions at $\sim$ 1 THz may pose some machining problems.

5 Conclusions

A novel full-waveguide band orthomode transducer has been designed. The design for the W-band has excellent matching, isolation and cross-polarization characteristics for the full design band of 75 – 110 GHz ($\sim$ 40% bandwidth). The design is simple to fabricate and assemble and is scalable to frequencies of $\sim$ 1 THz.

Research at the Five College Radio Astronomy Observatory is funded in part by a grant from the National Science Foundation.

6 References

[1] E. Wollack, "A Full Waveguide Band Orthomode Junction", Electronics Division Internal Report, National Radio Astronomy Observatory, Green Bank, WV, no. 303, May 1996.

[2] G. Narayanan, N. R. Erickson, and R. M. Grosslein, "Low Cost Direct Machining of Terahertz waveguide Structures," Tenth International Symposium on Space Terahertz Technology, pp. 518-528, Mar. 99.

[3] C. K. Walker, G. Narayanan, A. Hungerford, T. Bloomstein, S. Palmacci, M. Stern, J. Curtin, J., "Laser Micromachining of Silicon: A New Technique for Fabricating TeraHertz Imaging Arrays", Astronomical Telescopes and Instrumentation, SPIE Symposium, Kona, Hawaii, 1998.

[4] C. K. Walker, G. Narayanan, T. M. Bloomstein, "Laser Micromachining of Silicon: A New Technique for Fabricating Terahertz Waveguide Components", 1997, 8th International Symposium on Space Terahertz Technology, eds. Blundell and Tong, Harvard University.

[5] Bϕifot, A. M., Lier, E., and Schaug-Pettersen, T., "Simple And Broadband Orthomode Transducer", 1990, Proc. IEE, vol. 137, no. 6, pp 396-400.

[6] Bϕifot, A. M., "Classification of Orthomode Transducers", 1991, European Transactions on Telecommunication and Related Technologies, vol 2, no. 5, pp 503-510.

[7] Chattopadhyay, G., Philhour, B., Carlstrom, J. E., Church, S. Lange, A., and Zmuidzinas, J., "A 96 GHz Orthomode Transducer For Polatron", 1998, IEEE Microwave and Guided Wave Letters, vol 8., no. 12, pp 421-423.

[8] Montgomery, C. G., Dicke, R. H., and Purcell, E. M., "Principles of Microwave Circuits", Dover Publications, New York, 1948, pp. 459-466.

[9] Computer Simulation Technology (CST) Microwave Studio (MWS) v3.4, CST of America, Inc., Wellesley MA.

[10] High Frequency Structure Simulator (HFSS), v 5.6, Agilent Technology Inc., Palo Alto, CA.

[11] Advanced Design System (ADS), v2001, Agilent Technology Inc., Palo Alto, CA.

[12] Kerr, A. R., "Elements for E-Plane Split-Block Waveguide Circuits", 2001, ALMA Memo Series No. 381, NRAO.

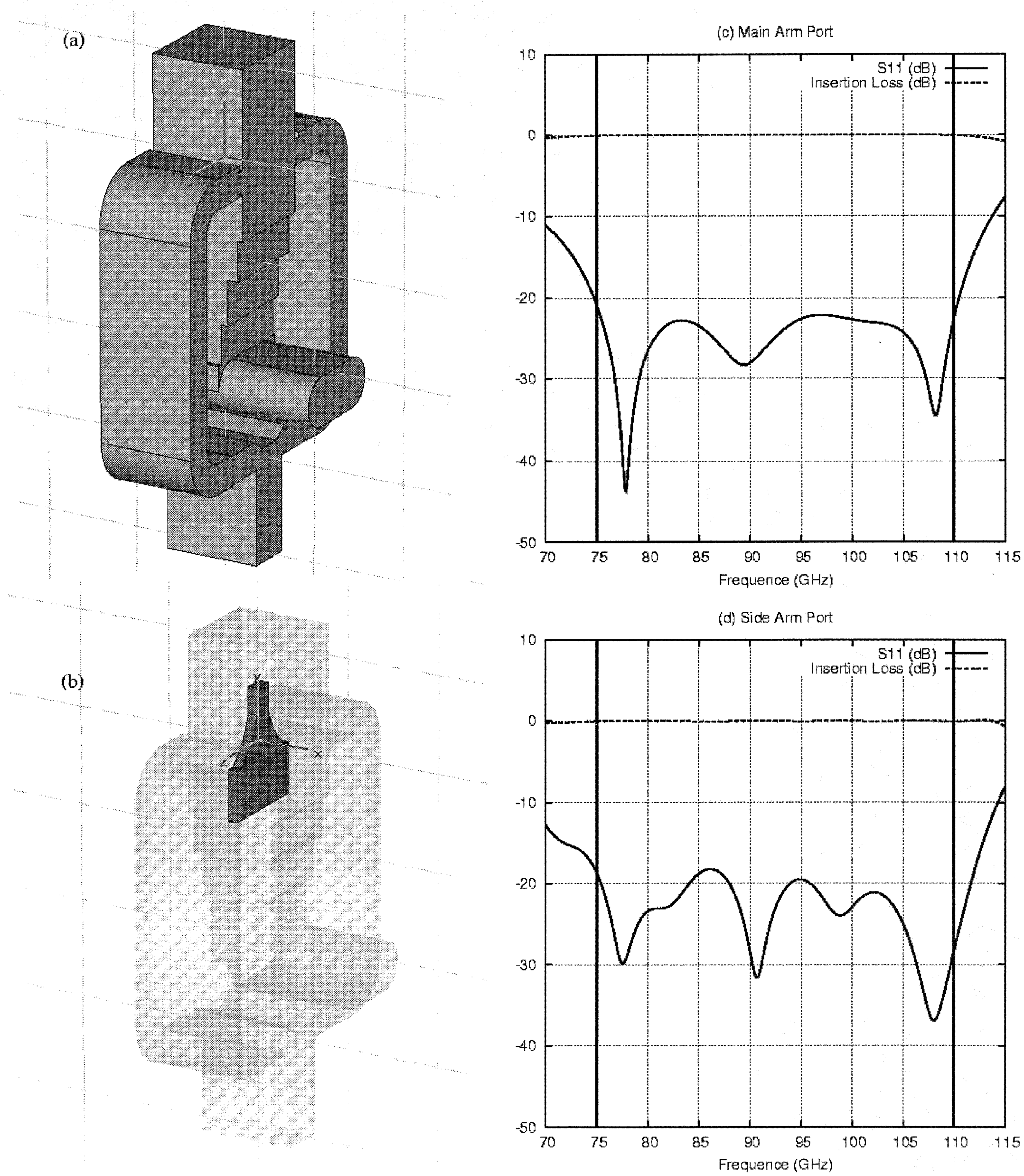

Figure 6: The full Orthomode Transducer. (a) Isometric view from the outside. The waveguide features of the OMT block measure $13.2 \times 7.6 \times 2.54$ mm. (b) Inside view showing the septum resting in the split block plane. (c) Simulated performance for the full structure for the main arm polarization. (d) Same as (c) for the side arm polarization port.